THERMAL ENERGY EFFECT ON OPTOELECTRONIC CHARACTERISTICS OF InGaAsN/GaAs LASER DIODE UNDER THE VARIATION OF QUANTUM WELL NUMBER

by

Mohammed Saad AL-GHAMDI*

Department of Physics, King Abdulaziz University, Jeddah, Saudi Arabia

Original scientific paper
https://doi.org/10.2298/TSCI22S1365A

A laser device based on InGaAsN quantum well active regions emitting at 1.26 μm is reported. The performances of the laser under the effect of thermal energy are investigated in terms of threshold current, I_{th}, gain parameter, $_{gt}$, photon energy, hν, and cavity length, L_c. Four structures with one, two, and three quantum wells along with a structure that have three quantum wells with tensile strained barriers are proposed to study the relation between the peak gain, g_{peak}, and photon energy. The founds show that structures with one and two quantum wells operating at room temperature and under pulse wave condition, exhibit a linear dependence of g_{peak} on both L_c and photon energy. It is shown that the threshold current density, J_{th}, increases at any temperature with the cavity length L_c ranging from 250 nm to 1000 nm. Also, the investigation of the proposed structures shows that g_t decreases with increasing temperature, while the ratio of the current density parameter to internal efficiency, J_t/η_i, per well increases with the quantum well number. A comparison was carried out for two particular structures with three quantum wells and GaAsP barriers, the results show a decrease in the threshold current per well.

Keywords: *thermal energy, optical gain, threshold current density, quantum well, semiconductor lasers*

Introduction

The InGaAsN materials have attracted considerable interests and been under intensive studies due to their potential daily life applications [1, 2]. The prior work on this class of materials was reported more than 20 years ago by Kondow *et al.* [3] has led to large variety of optoelectronic and photonic devices such as, diode lasers, filters, high electron mobility transistors and [4, 5].

The InGaAsN hydride system is composed of III-V elements group, because the bandgap energy is low; the structure has attracted many works for long wavelength laser diode emitting around 1300 nm applications. The superb high electron confinement in GaInNAs material systems has resulted in improved high-temperature performance. In addition, the use of GaInNAs as an alternative material system [6-9] offers cost effective production on large-scale GaAs substrates also medical and biomedical applications [10]. The initial results of the

* Author's e-mail: msalghamdi@kau.edu.sa

In GaAsN quantum well lasers (QW) were primarily obtained from materials grown by molecular beam epitaxy, however the progress in metal organic vapour phase epitaxy (MOCVD) materials grown have resulted in state-of-the-art 1300 nm emitting InGaAsN QW lasers in the past decades [11, 12]. The InGaAsN structure is grown on n^+ GaAs by MOCVD epitaxy.

The progress in highly strained InGaAsN QW lasers has also enabled the access of 1240 nm diode lasers without the need of nitrogen incorporation [13]. Advances in materials fabrication techniques have allowed the growth of GaInNAs material system with high quality by MOVPE.

The optical characteristics of GaInNAs/GaAs quantum well lasers in this reported work are investigated. The experimental system that have been used in this study is capable of measuring the light-current, optical gain and current-voltage characteristics of laser diodes over a wide temperature range. Also, the lasing wavelength at room temperature can be measured and determined.

Experimental details

All structures were grown by IQELTD, which is a leading merchant supplier of GaAs-based MQW edge emitting and vertical cavity laser wafers grown by metal-organic vapour phase epitaxy (MOVPE). During the process of the experimental growth, the design features for the reactor are low pressure (0.2 atmosphere) operation, high substrate rotating rates and room temperature.

Further processing into oxide stripe laser devices was done by clean room facility at Cardiff University. In the following a typical laser is presented where the details are given with the appropriate experimental results.

In fig. 1 a typical stripe laser is shown. The waveguide core consists of In(x)GaAs(y)N quantum well and a barrier with GaAs. The cladding layer made of Al(x)GaAs which is p doped at upper and n doped at lower side of the barrier. A GaAs cap layer is on the top of the *p* cladding layer and the buffer layer is on the bottom of the *n*-

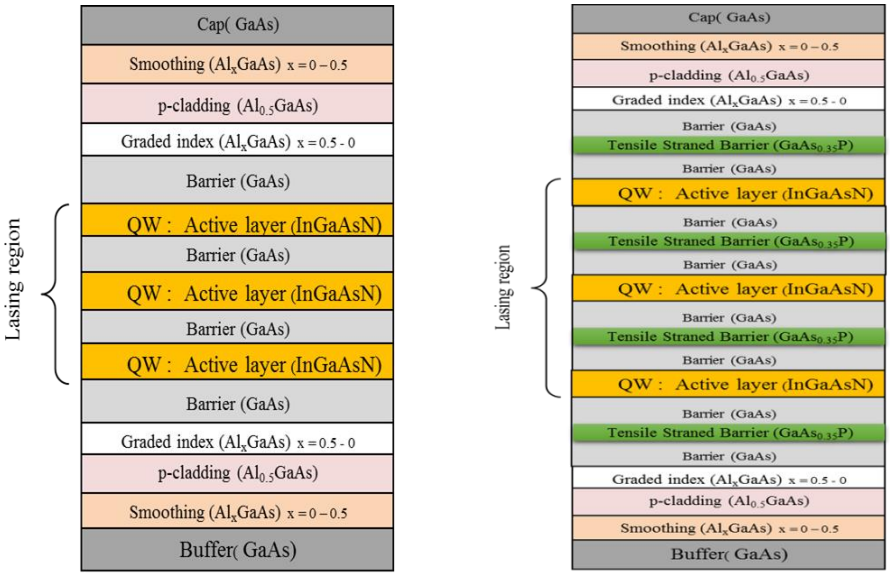

Figure 1. Typical structures for TQW and TQW + tensile strained barriers lasers

cladding layer. The structure is grown onto a GaAs substrate, which is 300 μm thick, before processing the layer of *n*-contact metallisation. The substrate has to be thin by a thinning process which reduces the thickness of the laser device structure to typically 100 μm. The ohmic contacts made to the device consist of AuGe-Ni-Au (*n*-metallisation) layer on the back and Au-Zn layer (*p*-metallisation) on the top. Inside the laser device there is a 50μm wide contact stripe, which made of Au-Zn, is in between the area where the injection current is confined by using the steps of this method.

It is also have been used that a process for cleaving the laser structures is used for the reason to have a determine length and width of the laser device, the width is the same for all used laser devices and not important as the length which can be different. The laser devices are used as cleaved, *i.e*. the length of the laser device is the actual cavity length, the reflectivities that take place in the laser device is due to the interface between the semiconductor and air, and there is no facet coating applied. The electromagnetic modes emit from both facets. The oxide stripe technique was chosen as it is easy to process [1].

In order to understand the thermal energy effect of on the optoelectronic characteristics of the proposed lasers under the variation of the quantum wells, we present four structures with single, two and three quantum wells and the fourth one with tensile strained barriers.

The SQW structure

We start by considering a structure with an active region consists of a single quantum well, which is composed of In(x)GaAs(y)N layer is typically 6.4 nm thick, and barriers consisting of 20 nm thick GaAs layers placed in each side of the quantum well. The cladding layers in this structure are of 1.2 μm thick Al(x)GaAs for each of them, which are doped with p and n that placed in the upper side and lower side of the barriers, respectively. The cap layer and the buffer layer are formed and used to decrease the contact resistance their thicknesses are 0.2 μm and 0.5 μm, respectively. The layers of SQW structure are provided in [14].

The DQW structure

This structure consists of an active region with a double quantum well, which is composed of a 6.4 nm thick In(x)GaAs(y)N layer each, and barriers formed of a 20 nm thick GaAs layers placed in between and in each side of the two quantum wells. The cladding layers in this structure are of 1.2 μm thick Al(x)GaAs for each of them, which are doped with *p* and *n* that placed in the upper side and lower side of the outer barriers, respectively. The cap and the buffer layers in this structure are as the same properties as SQW structure. The details of DQW structure are reported in [14].

The TQW structure

In this structure the active region consists of three quantum wells, which are composed of In(x)GaAs(y)N layers with 6.4 nm thicknesses, and GaAs barriers with a thickness of 20 nm. The GaAs layers are placed in between the three quantum wells and in each side of the two outer quantum wells. The cladding layers in this structure are of 1.2 μm thick Al(x)GaAs for each of them, which are doped with *p* and *n* that placed in the upper side and lower side of the outer barriers respectively. The cap and the buffer layers in this structure are as the same properties as SQW structure. The structural parameters of TQW structure are provided in [14].

The TQW + tensile strained barriers structure

This structure consists of an active region with triple quantum wells, which are made of In(x)GaAs(y)N layers of 6.4 nm thick. The barriers consist of GaAs layers and are 7 nm

thick, placed in each side of the three quantum wells. In addition barriers of GaAs(x)P layers of 8 nm and 12 nm thick, are placed in between the inner and the outer side of the GaAs barriers, respectively. Another barrier of GaAs layers, which consists of a 35 nm thick, is placed at the outer side of GaAs(x)P barriers. The cladding layers in this structure are Al(x)GaAs of 1.2 μm thick, which are doped with *p* and *n* that placed in the upper side and lower side of the barriers, respectively. The cap and the buffer layers in this structure are as the same properties as SQW structure. The details of layers of TQW + tensile strained barriers structure are provided in [14].

Results and dissection

First, begin by investigating the effect of thermal energy on the light-current characteristic for the SQW structure with one single QW, a cavity length of 436 μm. The can be done by varying the temperature from 160 K to 400 K, the result is illustrated in fig. 2. From this figure, the output light remains constant equal zero below certain values of the current until the lasing point is reached then it increases rapidly with current. The critical value corresponds to the threshold current, which can be found by drawing a straight line to the data of light-current characteristics. The interception of this line with the current axis defines the threshold current I_{th}.

Extensive works on temperature effects and current injection efficiency reported in [15] have demonstrated the importance of carrier leakage via thermionic carrier escape process in InGaAsN QW lasers [16].

Next, evaluate the threshold current density which is defined as:

$$J_{\text{th}} = \frac{I_{\text{th}}}{A} \tag{1}$$

where A is the product of the device length L_c and the oxide stripe width w, which is 50 μm, assuming that no correction has been made for current spreading. The light-current (L-I) characteristic curves are used to evaluate the threshold current densities for the used device lasers, which were illustrated in fig. 2, can be evaluated using eq. (1). In fig. 3, the threshold current density with temperature for different cavity lengths is illustrated.

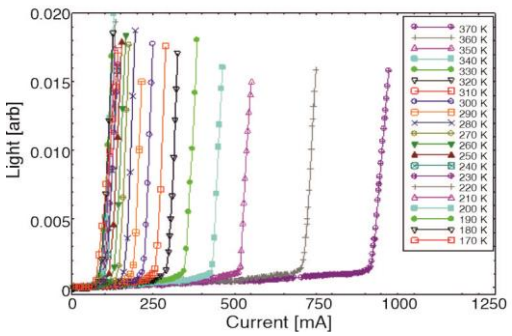

Figure 2. Illustration of light-current characteristic curves for SQW structure using a laser device with 436 μm cavity length for temperatures from 170 K up to 370 K.

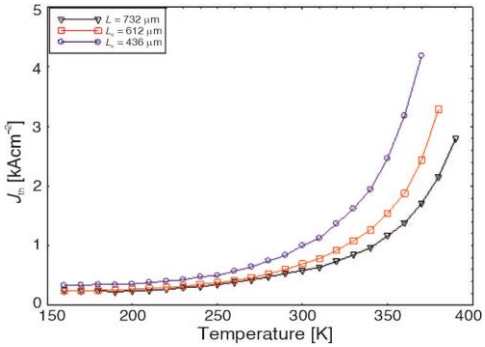

Figure 3. Threshold current densities as a function of temperature for SQW structure for different cavity lengths

It is shown from this figure that J_{th} increases almost linearly with the temperature, T, in the range 150-300 K, for T > 300 K, the current density increases exponentially this is due the escaping of carriers from the quantum well to both the barriers and the cladding layers.

Also, and J_{th} increases as the cavity length decreases. This behaviour usually attributed to the increase of mirror losses per unit length as the device length became shorter.

Now the focus on the TQW + tensile strained barriers structure is taken place, the active region is same as TQW structure, while additional barriers are deposited, the current density I_{th} is performed and reported in fig. 4. From this figure, it is noticed that the threshold current density flattens showing a slow variation with temperature, especially for T < 240 K, while it increases almost linearly when temperature varies from 250 K to 400 K. Also, J_{th} shows presents same trend when the cavity length is L_c = 436 μm, 612 μm, and 732 μm. This trend shows high temperature insensitivity in this structure as compared to the one that does not contain strained barriers due to the high electron confinement in structure with strained barriers.

In order to determine the gain parameter g_t the logarithm for threshold current density is evaluated and given in:

$$\ln\left(J_{\text{th}}\right)=\left\{\frac{inR^{-1}}{N\Gamma_w g_t}\right\}\frac{1}{L_c}+\left\{\frac{\alpha_i}{N\Gamma_w g_t}+\ln\left(\frac{NJ_t}{\eta_i}\right)-1\right\} \tag{2}$$

where R is the mirror reflectivity, α_i – the internal loss per unit length, L_c – the cavity length, Γ_w – the optical confinement factor per well, N – the number of wells, η_i – the inefficiency of the active region, and (g_t, J_t) are a reference point which can be determined from the line pass across the origin to the Gain-current curves.

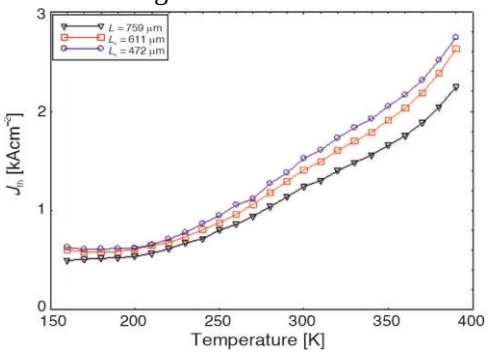

Figure 4. Threshold current densities as a function of temperature for TQW + tensile strained barriers structure at different cavity lengths

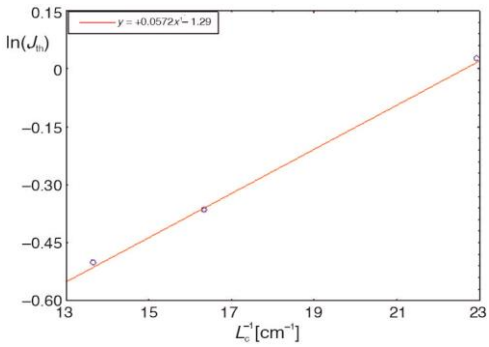

Figure 5. Plot of the logarithm for the threshold current density ln(J_{th}) against reciprocal cavity length L_c^{-1} at temperature 300 K for SQW structure

In fig. 5, the illustration of ln(J_{th}) *vs.* L_c^{-1} for a SQW structure at temperature of 300 K is shown. The plot of ln(J_{th}) is linear, where the evaluation of the slope of this curve to determine to find the parameter g_t,. Figure 6 shows the variation of ln(J_{th}) *vs.* L_c^{-1} for SQW, DQW, TQW, and TQW+ tensile strained barrier structures, the gain parameter for all structures are calculated and reported in tab. 1.

Table 1. Summary of gain parameter per well at temperatures of 300 K and 200 K for different device structures

Device structure	g_t per well [cm^{-1}] [300 K]	g_t per well [cm^{-1}] [200 K]
SQW structure	1569	2115
DQW structure	1742	2102
TQW structure	2177	1821
TQW + tensile strained barriers structure	1406	2145

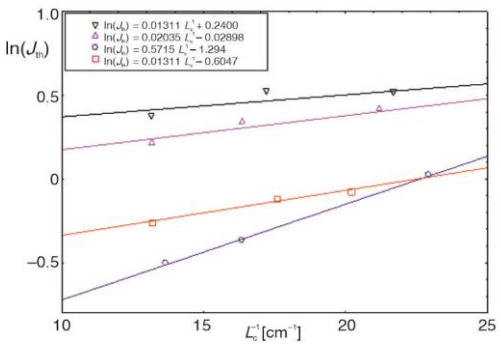

Figure 6. Plot of $\ln(J_{th})$ against L_c^{-1} at temperature 300 K for different laser structures; (○) for SQW structure, (□) for DQW structure, (▽) for TQW structure, and (Δ) for TQW + tensile strained barriers structure

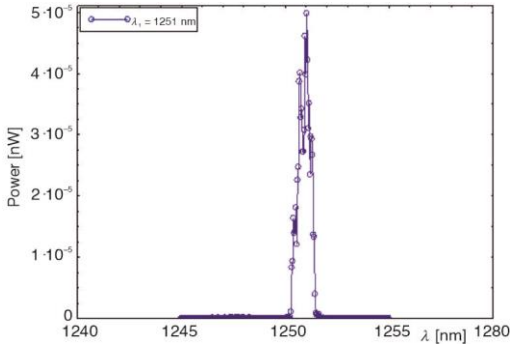

Figure 7. Lasing spectrum for SQW structure with cavity length of 732 μm at room temperature and with a driving current of 1.1 times the threshold current

From tab. 1 the final results of the gain parameter g_t per well for different device structures are listed. These results were calculated for SQW, DQW, TQW, and TQW+ tensile strained barriers structures at temperature of 200 K and 300 K. From these results one can say that g_t per well at any temperature for all structures are nearly the same within error, this means that it is independent on the well number of the structure at any temperature because g_t has been evaluated per well so all wells have the same properties such as the well width.

Next, the spectral output power against wavelength for SQW structure with cavity length of 732 μm and DQW structure with cavity length of 495 μm are is illustrated in fig. 7 and fig. 8.

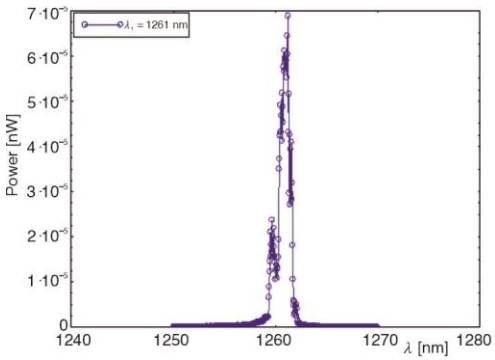

Figure 8. Lasing spectrum for DQW structure with cavity length of 495 μm at room temperature and with a driving current of 1.1 times the threshold current

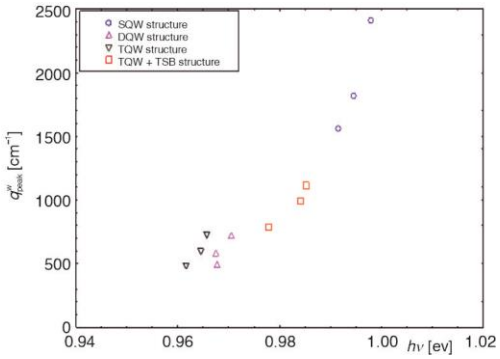

Figure 9. Plot of the peak gain per well against photon energy for different laser structures at room temperature; (○) for SQW structure, (□) for DQW structure, (▽) for TQW structure, and (Δ) for TQW + tensile strained barriers structure

These plots are measured at room temperature with a driving current above threshold by 10% of the threshold current. From these figures, the lasing wavelengths are evaluated to be 1251 nm and 1261 nm, respectively.

In order to understand the influence of the photon energy on lasing wavelengths in each structure, we evaluate the peak gain, which is defined as the g_{peak} per well. Figure 9

shows that g^{w}_{peak} increases with increasing $h\nu$, also, the increase of g^{w}_{peak} with the decrease of N means that one quantum well needs higher g^{w}_{peak} as compared to two quantum wells because g_{peak} is distributed on the two wells leaving a lower value of g_{peak} for each well. The reason for the increase of $h\nu$ with g^{w}_{peak} is that the value of the separation for the quasi-Fermi level, ΔE_f, determines g^{w}_{peak}, and the increase in ΔE_f results in an increase in $h\nu$. The increasing of ΔE_f will enhance the gain to be expanded over a photon energy range and that absolutely will cause an increase in g^{w}_{peak}.

Conclusion

We have reported the study of thermal energy on laser device structures based on various quantum well numbers, four particular structures with one, two, three quantum wells and three quantum wells + tensile strained barriers are proposed. The threshold current, the gain and the lasing wavelength of the laser are investigated in details under the influence of thermal energy. It is shown that the threshold current increases dramatically with the cavity length for a wide range of temperature. It is also found that the threshold current increases with the quantum wells number. Temperature insensitivity is higher in structure that contains strained barriers. The peak gain per well increases with increasing phton energy. It is also increase with the decrease of quantum well number means that structures with lower quantum wells needs higher peak gain per well as compared to structures with lower quantum wells where the peak gain is distributed on the high number of wells leaving a lower value of peak gain for each well.

Acknowledgment

The author thanks the Deanship of Scientific Research (DSR) at King Abdulaziz University, Jeddah, Saudi Arabia for technical and financial support under grant no. (J-1436-130 -38).

References

[1] Welch, D. F., *et al*., High-Power, 8 W CW Single-Quantum-Well Laser Diode Array, *Electronics Letters, 24* (1988), Jan., pp. 113-115
[2] Ferguson, J. W., *et al*., Optical Gain in GaInNAs and GaInNAsSb Quantum Wells, *IEEE Journal of Quantum Electronics, 47* (2011), 6, pp. 870-877
[3] Kondow, M., *et al*., A Novel Material of GaInNAs for Long-Wavelength-Range Laser Diodes with Excellent High-Temperature Performance, *Proceedings*, Int. Conf. on Solid State Device and Materials, Osaka, Japan, 1995, pp. 1016-1018
[4] Donnelly, J. P. Two-Dimensional Surface-Emitting Arrays of GaAs/AlGaAs Diode Lasers, *Lincoln Laboratory Journal, 3* (1990), Jan., pp. 361-384
[5] Taylor, R. J. E., *et al*. Electronic Control of Coherence in a Two-Dimensional Array of Photonic Crystal Surface Emitting Lasers, *Scientific Reports, 5* (2015), Aug., 13203
[6] Krysa, A. B., *et al*., InAsP/AlGaInP/GaAs QD Laser Operating at ~770 nm, *Journal of Physics: Conference Series., 740* (2016), 1, 012008
[7] Porsche, J., *et al*. Growth of Self-Assembled Inp Quantum Islands for Red-Light-Emitting Injection Lasers, *IEEE Journal of Selected Topics in Quantum Electronics, 6* (2000), 3, pp. 3482-3490
[8] Walter, G., *et al*., Coupled InP Quantum-Dot Ingap Quantum Well InP–InGaP–In (AlGa) P–InAlP Heterostructure Diode Laser Operation, *Applied Physics Letters, 79* (2001), 20, pp. 3215-3217
[9] Su, X.-B., *et al*., Elimination of Bimodal Size in InAs/GaAs Quantum Dots for Preparation of 1.3-μm Quantum Dot Lasers, *Nanoscale Research Letters, 13* (2018), 1, pp. 1-6
[10] Zhukov, A. E., *et al*., Lasing at 1.5 μm in Quantum Dot Structures on GaAs Substrates, *Semiconductors, 37* (2003), 12, pp. 1411-1413

[11] Tansu, N., *et al*., High-Performance 1200-nm InGaAs and 1300-nm InGaAsN Quantum-Well Lasers by Metalorganic Chemical Vapor Deposition, *IEEE Journal of Selected Topics in Quantum Electronics, 9* (2003), 5, pp. 1220-1227
[12] Tansu, N., *et al*., Physics and Characteristics of High Performance 1200 nm InGaAs and 1300–1400 nm InGaAsN Quantum Well Lasers Obtained by Metal–Organic Chemical Vapour Deposition, *Journal of Physics: Condensed Matter, 16* (2004), 31, S3277
[13] Tansu, N., *et al*., Extremely Low Threshold-Current-Density Ingaas Quantum-Well Lasers with Emission Wavelength of 1215–1233 nm, *Applied Physics Letters, 82* (2003), 23, pp. 4038-4040
[14] Blood, P., Gain and Recombination in Quantum Dot Lasers, *IEEE Journal of Selected Topics in Quantum Electronics, 15* (2009), 3, pp. 808-818
[15] Tansu, N., Luke, J. M., Current Injection Efficiency of InGaAsN Quantum-Well Lasers, *Journal of Applied Physics, 97* (2005), 5, 054502
[16] Xu, L., *et al*., Experimental Evidence of the Impact of Nitrogen on Carrier Capture and Escape Times in InGaAsN/GaAs Single Quantum Well, *IEEE Photonics Journal, 4* (2012), 6, pp. 2262-2271

Paper submitted: October 5, 2022
Paper revised: November 15, 2022
Paper accepted: November 20, 2022